Available online at www.sciencedirect.com
SCIENCE DIRECT®
Chaos, Solitons and Fractals 22 (2004) 653–668
CHAOS SOLITONS & FRACTALS
www.elsevier.com/locate/chaos

Chaos control in a nonlinear pendulum using a semi-continuous method

Francisco Heitor I. Pereira-Pinto [a], Armando M. Ferreira [a], Marcelo A. Savi [b,*]

[a] *Department of Mechanical and Materials Engineering, Instituto Militar de Engenharia, Rio de Janeiro, RJ 22.290.270, Brazil*
[b] *COPPE - Department of Mechanical Engineering, Universidade Federal do Rio de Janeiro, Caixa Postal 68.503, Rio de Janeiro, RJ 21.945.970, Brazil*

Accepted 2 March 2004

Abstract

Chaotic behavior of dynamical systems offers a rich variety of orbits, which can be controlled by small perturbations in either a specific parameter of the system or a dynamical variable. Chaos control usually involves two steps. In the first, unstable periodic orbits (UPOs) that are embedded in the chaotic set are identified. After that, a control technique is employed in order to stabilize a desirable orbit. This contribution employs the close-return method to identify UPOs and a semi-continuous control method, which is built up on the OGY method, to stabilize some desirable UPO. As an application to a mechanical system, a nonlinear pendulum is considered and, based on parameters obtained from an experimental setup, analyses are carried out. At first, it is considered signals generated by numerical integration of the mathematical model. After that, the analysis is done from scalar time series and therefore, it is important to evaluate the effect of state space reconstruction. Delay coordinates method is employed with this aim. Finally, an analysis related to the effect of noise in controlling chaos is of concern. Results show situations where these techniques may be used to control chaos in mechanical systems.

1. Introduction

Chaotic behavior has been extensively analyzed in different fields of sciences as for example engineering, medicine, ecology, biology and economy. As a matter of fact, chaos may occur in many natural processes and the idea that chaotic behavior may be controlled by small perturbations of some physical parameter is making this kind of behavior to be desirable in different applications.

Chaos control is based on the richness of responses of chaotic behavior. A chaotic attractor has a dense set of unstable periodic orbits (UPOs) and the system often visits the neighborhood of each one of them. Moreover, chaotic response has sensitive dependence to initial condition, which implies that the system's evolution may be altered by small perturbations. Therefore, chaos control may be understood as the use of tiny perturbations for the stabilization of an UPO embedded in a chaotic attractor, which makes this kind of behavior to be desirable in a variety of applications, since one of these UPO can provide better performance than others in a particular situation. It should be pointed out that it is not necessary to have a mathematical model to achieve the control goal since all control parameters may be resolved from time series analysis.

Chaos control methods may be classified as discrete or continuous techniques. The first chaos control method had been proposed by Ott et al. [30], nowadays known as the OGY (Ott–Grebogi–Yorke) method. This is a discrete

* Corresponding author.
E-mail addresses: heitor@epq.ime.eb.br (F.H.I. Pereira-Pinto), armando@epq.ime.eb.br (A.M. Ferreira), savi@ufrj.br (M.A. Savi).

0960-0779/$ - see front matter © 2004 Elsevier Ltd. All rights reserved.
doi:10.1016/j.chaos.2004.02.047

technique that considers small perturbations promoted in the neighborhood of the desired orbit when the trajectory crosses a specific surface, such as some Poincaré section. On the other hand, continuous methods are exemplified by the so called delayed feedback control, proposed by Pyragas [35], which states that chaotic systems can be stabilized by a feedback perturbation proportional to the difference between the present and a delayed state of the system. Recently, Wang and Jing [51] exploits a Lyapunov function method as an alternative for chaos control in a nonlinear pendulum.

There are many improvements of the OGY method that aim to overcome some of its original limitations, as for example: control of high periodic and high unstable UPO [22,29,36] and control using time delay coordinates [15,24,45]. For more details on chaos control based on OGY method refer to [2,3,5,6,13,14,16,20,28,42]. Moreover, there are reports on some experimental applications of OGY based control methods as in magnetoelastic ribbons [12,22,23], in nonlinear pendulums [22,24,47,49] and in a double pendulum [7].

The main purpose of this contribution is the analysis of chaos control in a nonlinear pendulum that is based on the experimental apparatus previously analyzed by Franca and Savi [18] and Pinto and Savi [32]. This pendulum has both torsional stiffness and damping. All signals are generated numerically by the integration of the equations of the mathematical model proposed, which uses experimentally identified parameters. The close-return (CR) method [1] is employed to determine the UPO embedded in the attractor. A variation of the OGY technique called semi-continuous control (SCC) method, proposed by Hübinger et al. [22] and extended by Korte et al. [24], is considered to stabilize the desirable orbit. The control analysis considers two different situations: all state variables are available; and just a scalar time series is available. For the second situation, state space reconstruction is done with the method of delay coordinates [48]. Since experimental data is associated with noise contamination, which is unavoidable in cases of data acquisition, the effect of noise in control techniques is an important point to be analyzed. The robustness of control procedure is an essential aspect to the controllability of a dynamical system. Therefore, the effect of noise in the controlling procedures is analyzed, defining some limitations of these techniques. Results confirm the possibility of the use of this approach to deal with mechanical systems.

2. Determination of unstable periodic orbits

The control of chaos can be treated as a two-stage process. The first stage is composed by the identification of UPO and is named as ''learning stage''. Since UPO are system invariants, they can be analyzed from phase space reconstructed from a scalar time series [21].

This article considers the close-return (CR) method [1] for the detection of UPO embedded in the attractor. The basic idea is to search for a period-P UPO in the time series represented by vectors $\{u_i\}_{i=1}^{N}$. This state vector may be obtained by state space reconstruction from a scalar time series s_n $(n = 1, \ldots, N)$ using delay coordinates, for example [48]. The identification of a period-P UPO is based on a search for pairs of points in the time series that satisfy the condition $|u_i - u_{i+P}|_{i=1}^{(N-P)} \leqslant r_1$ where r_1 is the tolerance value for distinguishing return points. After this analysis, all points that belong to a period-P cycle are grouped together. During the search, the vicinity of a UPO may be visited many times, and it is necessary to distinguish each orbit, remove any cycle permutation and to average them in order to improve estimations as shown by Otani and Jones [29].

Other different approaches can be employed for the determination of UPO as proposed by Pawelzik and Schuster [31], Pierson and Moss [33], So et al. [46], Schmelcher and Diakonos [39,40], Diakonos et al. [11], Pingel et al. [34], Davidchack and Lai [8], Dhamala et al. [10].

After the identification of a UPO, one can proceed to the next stage of the control process that is the stabilization of the desired orbit. In the following section, it is presented one of the procedures used for this aim: the SCC control method.

3. Semi-continuous control method

The OGY [30] approach is described considering a discrete system of the form of a map $\xi_{i+1} = F(\xi_i, p)$, where $p \in \Re$ is an accessible parameter for control. This is equivalent to a parameter dependent map associated with a general surface, usually a Poincaré section. Let $\xi_F = F(\xi_F, p_0)$ denote the unstable fixed point on this section corresponding to an orbit in the chaotic attractor that one wants to stabilize. Basically, the control idea is to monitor the system dynamics until the neighborhood of this point is reached. After that, a proper small change in the parameter p causes the next state ξ_{i+1} to fall into the stable direction of the fixed point. In order to find the proper variation in the control parameter, δp, it is considered a linearized version of the dynamical system near the equilibrium point.

$$\delta\xi_{i+1} \cong A\delta\xi_i + w\delta p_i, \tag{1}$$

where $\delta\xi_i = \xi_i - \xi_F$, $\delta p_i = p_i - p_0$, $A = D_\xi F(\xi_F, p_0)$, and $w = \partial F/\partial p(\xi_F, p_0)$.

The OGY method can be employed even in situations where a mathematical model is not available. Under this situation, all parameters can be extracted from time series analysis. The Jacobian A and the sensitivity vector w can be estimated from a time series using a least-square fit method as described in [1,29].

In order to overcome some limitations of the original OGY formulation such as control of orbits with large instability, measured by unstable eigenvalues, and orbits of high period, Hübinger et al. [22] introduced a semi-continuous control (SCC) method or local control method, which description is presented as follows.

The SCC method lies between the continuous and the discrete time control because one can introduce as many intermediate Poincaré sections, viewed as control stations, as it is necessary to achieve stabilization of a desirable UPO. Therefore, the SCC method is based on measuring transition maps of the system. These maps relate the state of the system in one Poincaré section to the next.

In order to use N control stations per forcing period T, one introduces N equally spaced successive Poincaré sections $\Sigma_n, n = 0, \ldots, (N-1)$. Let $\xi_F^n \in \Sigma_n$ be the intersections of the UPO with Σ_n and $F^{(n,n+1)}$ be the mapping from one control station Σ_n to the next one Σ_{n+1}. Here, the superscript n is used instead of the subscript i of the OGY method, to differentiate both methods. Hence, one considers the map

$$\xi_F^{n+1} = F^{(n,n+1)}(\xi_F^n, p^n). \tag{2}$$

A linear approximation of $F^{(n,n+1)}$ around ξ_F^n and p_0 is considered as follows:

$$\delta\xi^{n+1} \cong A^n\delta\xi^n + w^n\delta p^n, \tag{3}$$

where $\delta\xi^{n+1} = \xi^{n+1} - \xi_F^{n+1}$, $\delta p^n = p^n - p_0$, $A^n = D_{\xi^n}P^{(n,n+1)}(\xi_F^n, p_0)$, and $w^n = \frac{\partial P^{(n,n+1)}}{\partial p^n}(\xi_F^n, p_0)$.

Hübinger et al. [22] analyze the possibility of the eigenvalues of A^n be complex numbers and then they use the fact that the linear mapping A^n deforms a sphere around ξ_F^n into an ellipsoid around ξ_F^{n+1}. Therefore, a singular value decomposition (SVD),

$$A^n = U^n W^n (V^n)^T = \{\, u_u^n \quad u_s^n \,\} \begin{bmatrix} \sigma_u^n & 0 \\ 0 & \sigma_s^n \end{bmatrix} \{\, v_u^n \quad v_s^n \,\}^T \tag{4}$$

is employed in order to determine the directions v_u^n and v_s^n in Σ_n which are mapped onto the largest, $\sigma_u^n u_u^n$, and shortest, $\sigma_s^n u_s^n$, semi-axis of the ellipsoid in Σ_{n+1}, respectively. Here, σ_u^n and σ_s^n are the singular values of A^n.

Korte et al. [24] establish the control target as being the adjustment of δp^n such that the direction v_s^{n+1} on the map $n+1$ is obtained, resulting in a maximal shrinking on map $n+2$. Therefore, it demands $\delta\xi^{n+1} = \alpha v_s^{n+1}$, where $\alpha \in \Re$. Hence, from Eq. (3) one has that

$$A^n\delta\xi^n + w^n\delta p^n = \alpha v_s^{n+1}, \tag{5}$$

which is a relation from what α and δp^n can be conveniently chosen.

3.1. State space reconstruction using delay coordinates

When only a scalar time series is available for measurements, one needs to convert the observations into state vectors. This task is known as state space reconstruction. As shown by Dressler and Nitsche [15], state space reconstruction by delay coordinates leads to a map $F^{(n,n+1)}$ that will depend on all parametric changes that influence the system in the time interval $t^n - \tau \leqslant t \leqslant t^n$, that is, $\delta p^n, \delta p^{n-1}, \ldots, \delta p^{n-r}$ with r being the largest integer value such that δp^{n-r} lies in this interval. Hence, the use of delay coordinates implies that the following map is considered, instead of the one shown in Eq. (2):

$$\xi_F^{n+1} = F^{(n,n+1)}(\xi_F^n, \delta p^n, \delta p^{n-1}, \ldots, \delta p^{n-r}). \tag{6}$$

Taking the linear approximation of $F^{(n,n+1)}$ around ξ_F^n and p_0 using deviation variables $\delta\xi^{n+1} = \xi^{n+1} - \xi_F^{n+1}$:

$$\delta\xi^{n+1} \cong A^n\delta\xi^n + B_0^n\delta p^n + B_1^n\delta p^{n-1} + \cdots + B_r^n\delta p^{n-r}, \tag{7}$$

where, $A^n = D_{\xi^n}F^{(n,n+1)}(\xi_F^n, \delta p^n, \delta p^{n-1}, \ldots, \delta p^{n-r})$ and $B_i^n = D_{\delta p^{n-i}}F^{(n,n+1)}(\xi_F^n, \delta p^n, \delta p^{n-1}, \ldots, \delta p^{n-r})$.

SVD procedure is employed again and the resulting linear system is given by:

$$A^n\delta\xi^n + B_0^n\delta p^n + B_1^n\delta p^{n-1} + \cdots + B_r^n\delta p^{n-r} = \alpha v_s^{n+1}, \tag{8}$$

from what α and δp^n can be conveniently calculated. All the local dynamical properties of the control points can be extracted from state space reconstruction and one must wait until the system dynamics reaches the neighborhood of any of them to adequately perturb the control parameter.

In the next section, a nonlinear pendulum is analyzed applying the CR method to search for UPO and the SCC method to perform control of this mechanical device.

4. Controlling a nonlinear pendulum

As a mechanical application of general chaos control procedures here presented, a nonlinear pendulum is considered. The motivation of the proposed pendulum is an experimental set up, previously analyzed by Franca and Savi [18] and Pinto and Savi [32]. Here, a mathematical model is developed to describe the dynamical behavior of the pendulum while the corresponding parameters are obtained from the experimental apparatus. Numerical simulations of such model are employed in order to obtain time series related to the pendulum response. Finally, some unstable periodic orbits are identified with the CR method and their control simulated employing the SCC method.

The considered nonlinear pendulum is shown in Fig. 1. The right side presents the experimental apparatus while the left side shows an schematic picture. Basically, pendulum consists of an aluminum disc (1) with a lumped mass (2) that is connected to a rotary motion sensor (4). A magnetic device (3) provides an adjustable dissipation of energy. A string-spring device (6) provides torsional stiffness to the pendulum and an electric motor (7) excites the pendulum via the string-spring device. An actuator (5) provides the necessary perturbations to stabilize this system by properly changing the string length.

In order to describe the dynamics of this pendulum, a mathematical model is proposed. Let F_1 andF_2 be the forces exerted on the rotating masses and given by:

$$F_1 = k\left(\sqrt{a^2 + b^2 - 2ab\cos(\varpi t)} - (a - b) - \frac{d}{2}\phi\right) \quad F_2 = k\left(\frac{d}{2}\phi - \Delta l\right), \tag{9}$$

where ϖ is the forcing frequency, a defines the position of the guide of the string with respect to the motor, b is the length of the excitation arm of the motor, D is the diameter of the metallic disc and d is the diameter of the driving pulley. The Δl parameter is the length variation in the string provided by the linear actuator (5) shown in Fig. 1(a). This

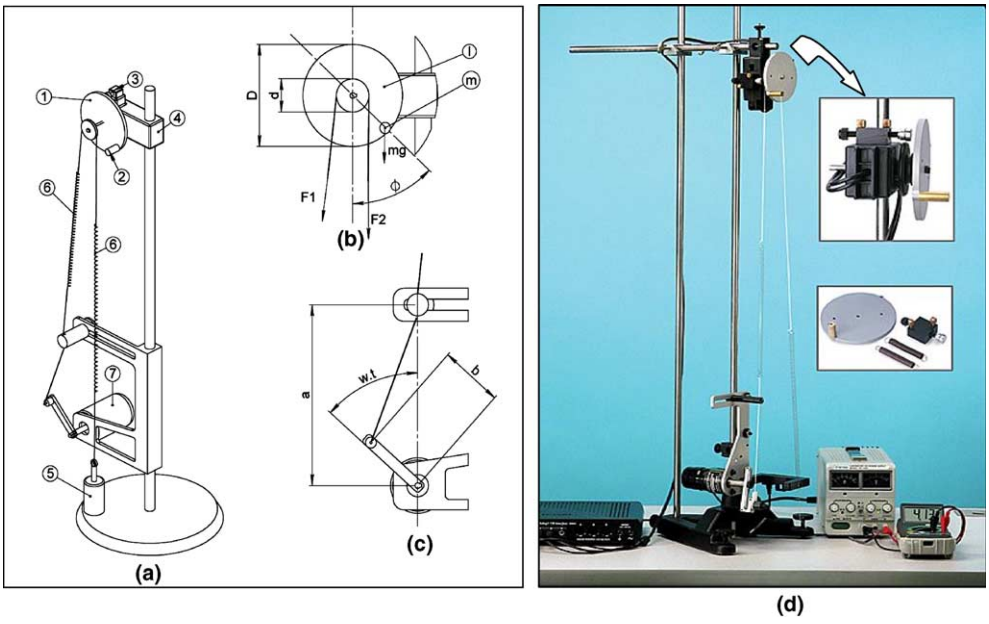

Fig. 1. Nonlinear pendulum. (a) Physical model. (1) Metallic disc; (2) Lumped mass; (3) Magnetic damping device; (4) Rotary motion sensor; (5) Actuator; (6) String-spring device; (7) Electric motor. (b) Parameters and forces on the metallic disc. (c) Parameters from driving device. (d) Experimental apparatus.

parameter is considered as the variation on the accessible parameter for control purposes. Therefore, the equation of motion is given by:

$$\begin{Bmatrix} \dot{\phi} \\ \ddot{\phi} \end{Bmatrix} = \begin{bmatrix} 0 & 1 \\ -\frac{kd^2}{2I} & -\frac{\zeta}{I} \end{bmatrix} \begin{Bmatrix} \phi \\ \dot{\phi} \end{Bmatrix} + \begin{Bmatrix} 0 \\ \frac{kd}{2I}\left[\sqrt{a^2+b^2-2ab\cos(\varpi t)} - (a-b) - \Delta l\right] - \frac{mgD}{2I}\sin(\phi) \end{Bmatrix}, \tag{10}$$

where I is the total inertia of rotating parts, m is the lumped mass and ζ is the dissipation parameter.

The determination of parameters in equation of motion is done by considering the experimental setup of Franca and Savi [18]. Table 1 shows the parameters that are evaluated from the experimental setup.

Values of the adjustable parameters ϖ and ζ are tuned to generate chaotic response in agreement to the experimental work done by Franca and Savi [18]. The Δl parameter has a null value for the system without control action. Therefore, using the parameters presented in Table 2, it is possible to use a fourth-order Runge–Kutta scheme in order to perform numerical simulations of the equations of motion. Fig. 2 shows temporal evolution, phase space and strange attractor related to this response. Notice that the system presents a chaotic response that can be assured evaluating Lyapunov exponents. By employing the algorithm proposed by Wolf et al. [52], one obtains the following spectrum that presents one positive value: $\lambda = \{+19.21, -5.19\}$.

The first stage of the control strategy is the identification of UPOs embedded in the chaotic attractor. The CR method [1] is employed with this aim, after dividing the coordinates ϕ and $\dot{\phi}$ by a factor 9 and 18, respectively. The value of the tolerance r_1 is chosen to be 0.003 and r_2 is set to be ten times r_1 Fig. 2(c) presents a strange attractor of the motion showing points in the Poincaré section corresponding to some identified UPOs that will be stabilized in the next stage of control strategy. The SCC method is applied considering three control stations (named intermediate Poincaré section #2, #3, #4). Fig. 3 shows these sections, also identifying the desirable UPOs. Therefore, a total of four maps per forcing period are considered.

After the identification of the UPOs embedded in the Poincaré section #1, the piercing of the same UPOs in the other three Poincaré sections is determined. Then, the local dynamics expressed by the Jacobian matrix and the sensitivity vector of the transition maps in a neighborhood of the fixed points are determined using the least-square fit method [1,29]. After that, the SVD technique is employed for determining the stable and unstable directions near the next fixed point. The sensitivity vectors are evaluated allowing the trajectories to come close to a fixed point and then

Table 1
Experimental values of parameters

a (m)	b (m)	d (m)	D (m)	I (kg m^4)	k (N/m)	m (kg)
1.6×10^{-2}	6.0×10^{-2}	2.9×10^{-2}	9.2×10^{-2}	1.876×10^{-4}	4.736	1.6×10^{-2}

Table 2
Values of adjustable parameters

ϖ (rad/s)	ζ (kg m^2/s)	Δl (m)
5.15	5.575×10^{-5}	0

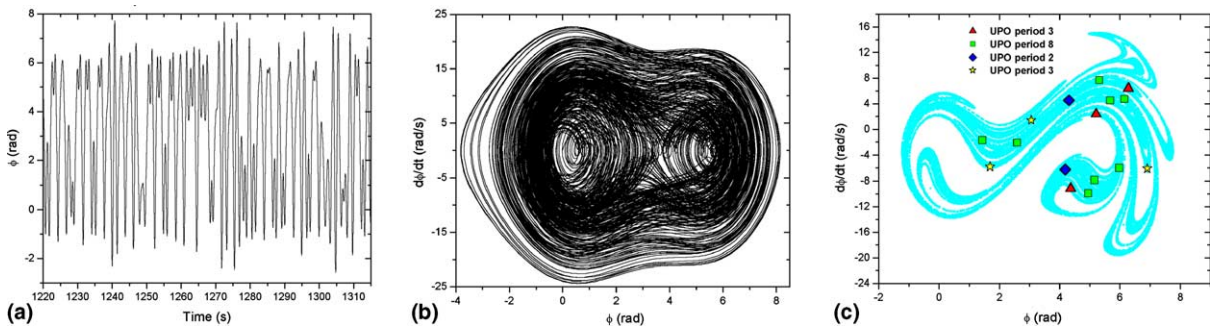

Fig. 2. Chaotic response. (a) Temporal evolution in 90 s. (b) Phase space. (c) Strange attractor.

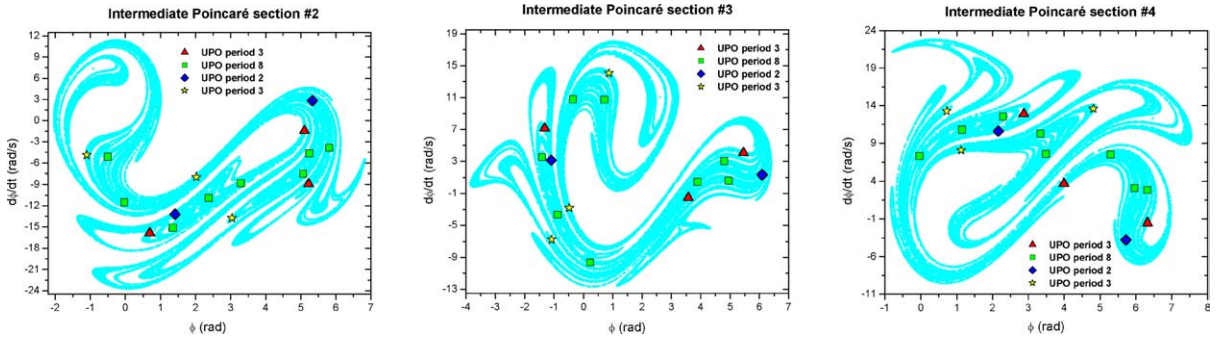

Fig. 3. Strange attractor in intermediate sections showing identified UPOs.

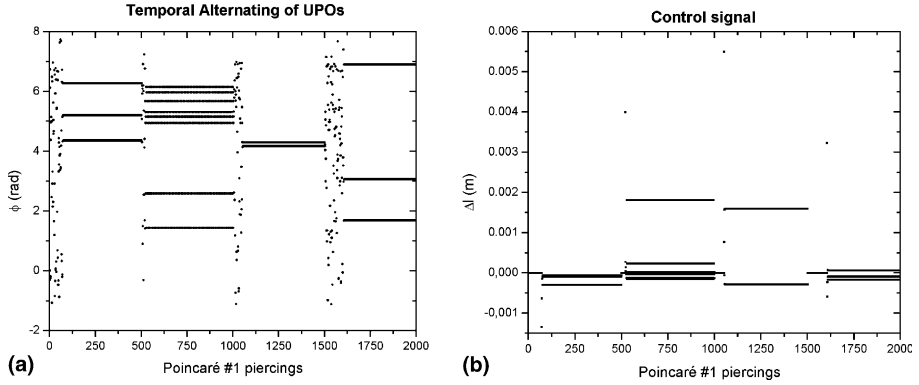

Fig. 4. Response under control. (a) Temporal alternating of UPOs in Poincaré section #1. (b) Control signal.

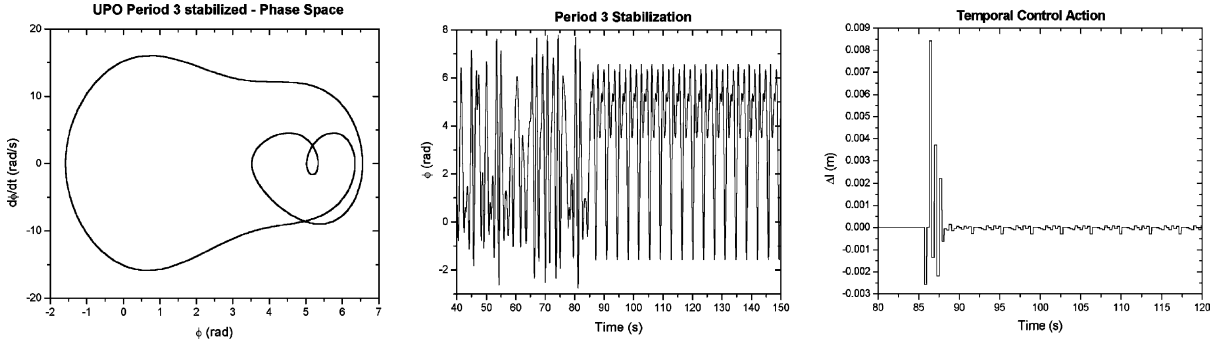

Fig. 5. UPO period-3 stabilized.

one perturbs the parameters by the maximum permissible value. In this case, a perturbation in $\Delta l_{\max} = 20$ mm is performed, fitting the resulting deviations $[\delta\xi^{n+1}(\Delta l) - A^n\delta\xi^n]/\Delta l$ from the next piercing by the least square procedure. After that, SCC method is employed to stabilize unstable periodic orbits and the parameter changes are calculated from Equation (5).

In order to explore the possibilities of alternating the stabilized orbits with small changes in the control parameter, one performs a simulation that aims the stabilization of the following UPOs: a period-3 UPO in the first 500 forcing periods, a period-8 UPO between 500 and 1000 forcing periods, a period-2 UPO between 1000 and 1500 forcing periods and a period-3 UPO, different from the first one, between 1500 and 2000 forcing periods. Fig. 4 shows the system's

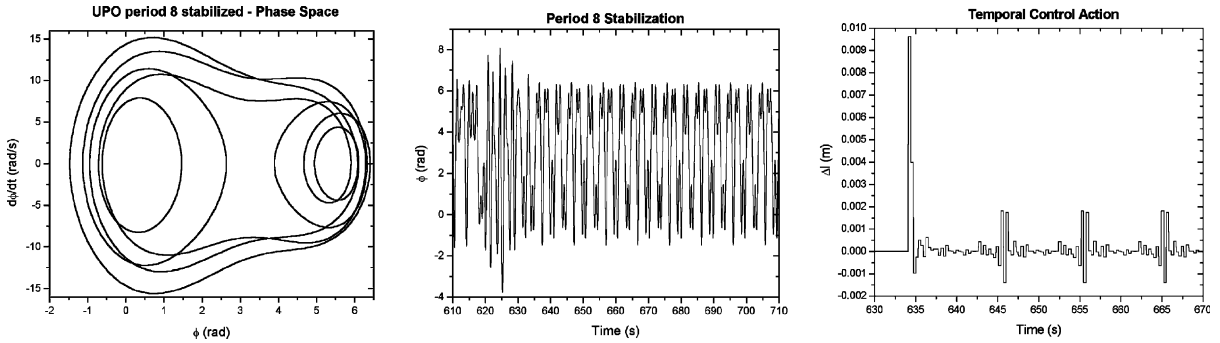

Fig. 6. UPO period-8 stabilized.

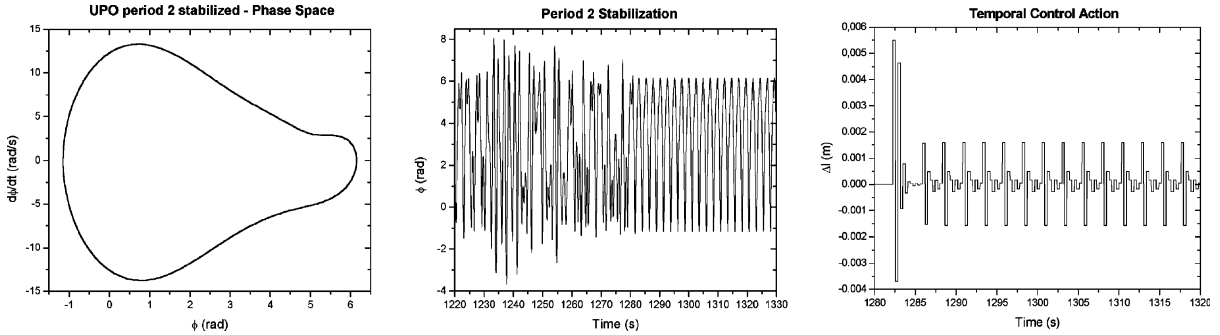

Fig. 7. UPO period-2 stabilized.

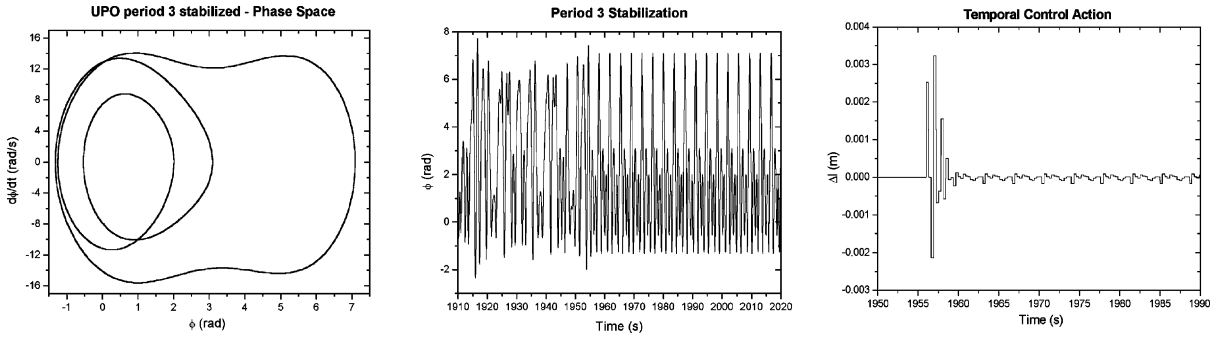

Fig. 8. UPO period-3 stabilized.

dynamics in the Poincaré section #1 during the actuation. Notice that different times are needed for the system to achieve the desired stabilization on a particular UPO. This happens because one must wait until the trajectory comes close enough to a control point to perform the necessary perturbation, exploiting the ergodicity property of the chaos behavior. Moreover, it should be pointed out that, as expected, results show that unstable orbits are stabilized with small variations of control parameter after a transient, less than 2 mm in this case.

More details on the orbits stabilized due to SCC method are presented in Figs. 5–8. In all cases, as the target orbit changes, one notes short transients on the temporal evolution of Δl followed by tiny periodic perturbations, as well as good results regarding to keeping the system in the desired orbit.

5. Controlling using delay coordinates

In this section, it is assumed that a scalar time series of angular position is acquired with sampling time Δt. Therefore, in order to reconstruct the dynamics of the system from time series, delay coordinates is employed. The average mutual information method is employed to determine time delay [19] while the false nearest neighbors method is used to estimate embedding dimension [37]. Fig. 9 shows times series, the reconstructed state space and Poincaré section related to chaotic behavior. State space reconstruction is considered with time delay $\tau = 24\Delta t$ and a embedding dimension $D_e = 2$ [18].

After the identification of the UPOs embedded in the Poincaré section #1, the piercing of the same UPO in the other three Poincaré sections is determined. Then, the local dynamics expressed by the Jacobian matrix of the transition maps are determined using the least-square method (LSM) [1]. The sensitivity vectors B_0^n and B_1^n are determined as proposed by Dressler and Nitsche [15]. Subsequently, the SVD technique is employed to determine stable and unstable directions near the next control point and the necessary perturbation on Δl parameter is done when the system's trajectory enters in a neighborhood of a control point.

In order to explore the possibilities of alternating the stabilized orbits with small changes in the Δl parameter, a simulation is performed aiming the stabilization of a sequence of UPO: period-3, period-6, period-4 and period-6 UPO different from the first one. Fig. 10 shows the system's position and parameter perturbation in the Poincaré section #1 during the control procedure. Notice that the control is turned on after the first 500 forcing periods. It is clear that the control procedure is also able to perform UPO stabilization using delay coordinates.

Figs. 11 and 12 show the first two stabilized orbits of the previous simulations, period-3 and period-6, respectively. As the target orbit is stabilized, one notes short transients on the temporal evolution of Δl followed by tiny periodic perturbations, as well as good results regarding to keeping the system in the desired UPO.

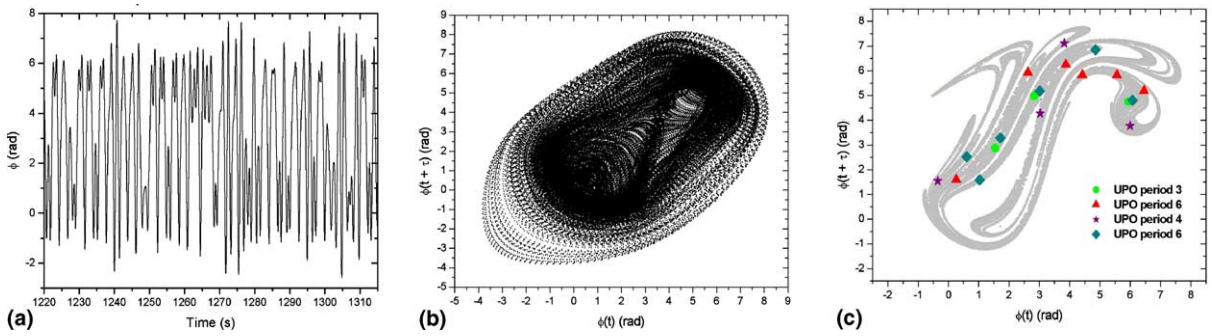

Fig. 9. (a) Temporal evolution in 90 s. (b) Phase space. (c) Strange attractor.

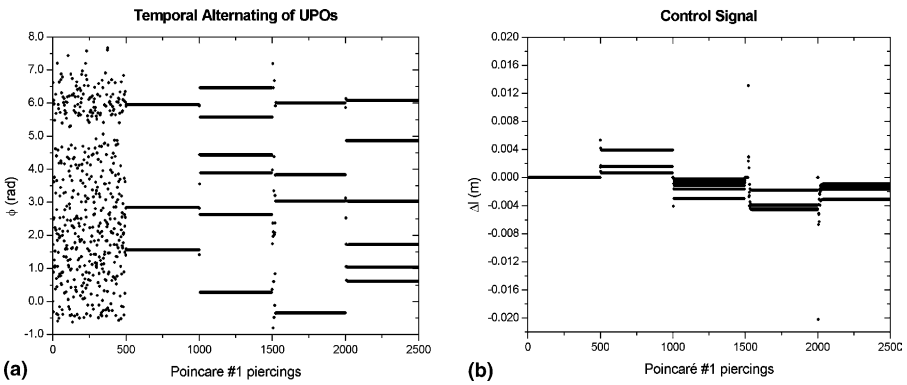

Fig. 10. Response under control. (a) Position of UPOs in Poincaré section #1. (b) Control signal.

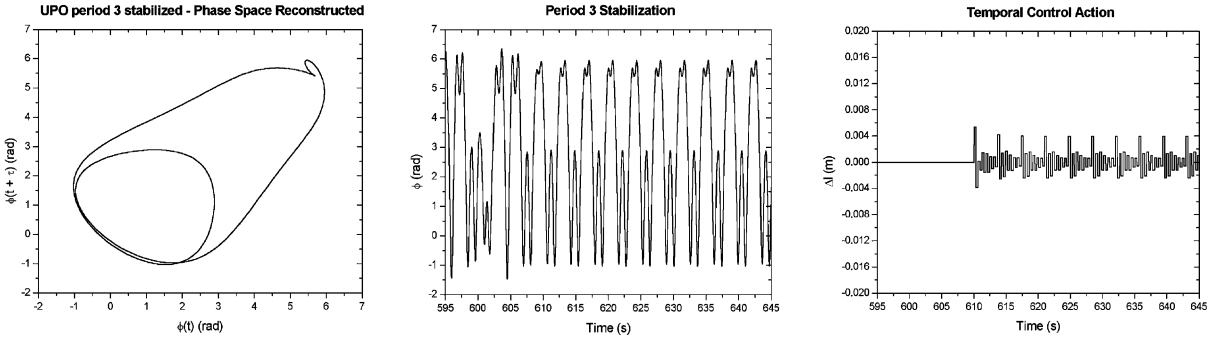

Fig. 11. UPO #1 stabilized.

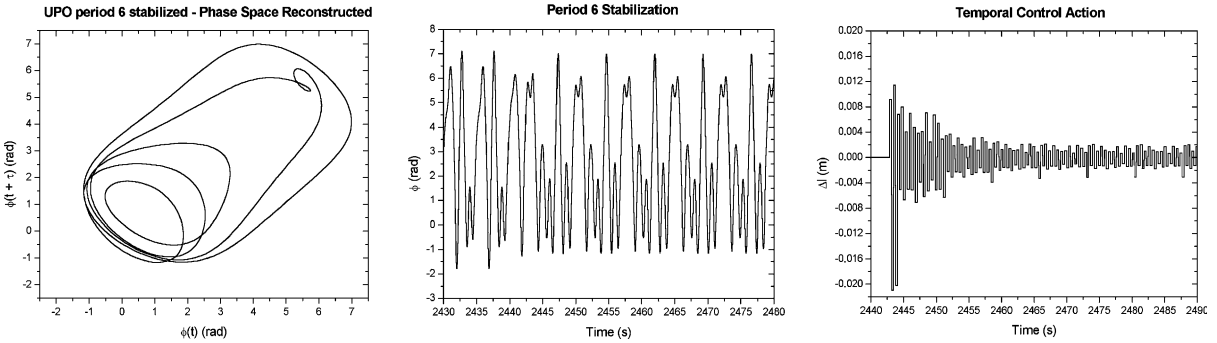

Fig. 12. UPO #4 stabilized.

6. Effect of noise on the control

Since noise contamination is unavoidable in cases of experimental data acquisition, it is important to evaluate its effect on chaos control procedures. Noise reduction schemes for chaotic noisy time series is an alternative [9,4,17,25,38,41,43,44] or Kalman filtering [26,27,50] but these subjects are beyond the scope of this paper. On the other hand, it is possible to employ robust control procedures to avoid filtering processes.

This section evaluates noise sensitivity of the chaos control technique discussed later. The analysis considers that all variables are known and therefore, it is not necessary to use state space reconstruction. Noise suppression is not considered and it is beyond the scope of this contribution the influence of noise on the determination of UPOs. For this analysis, see Refs. [33,46,54–56].

Ott et al. [30] say that the efficiency of the OGY method is close related to the noise level. Spano et al. [53] also study the effect of noise in OGY method, confirming the previous conclusion. This article investigates the effect of noise on the SCC method applied to a nonlinear pendulum verifying the influence on estimated parameters and on the system stabilization. Moreover, since SCC consider intermediate sections, it is also analyzed the effect of increasing the number of these control stations to compensate noise effects.

In order to simulate experimental noisy data sets, a white Gaussian noise is introduced in the signal, comparing results of control procedures with a clean time series, free of noise. In general, noise can be expressed as follows,

$$\begin{aligned} \dot{x} &= f(x,t) + \mu_{\mathrm{d}}, \\ z &= h(x,t) + \mu_{\mathrm{o}}, \end{aligned} \tag{11}$$

where x represents state variables, while z represents the observed response. On the other hand, μ_{d} and μ_{o} are, respectively, dynamical and observed noises. Notice that μ_{d} has influence on system dynamics in contrast with μ_{o}. The noise level is parameterized by the root mean square value of the clean signal ($\mathrm{RMS}_{\mathrm{signal}}$). Therefore, the noise probability distribution variance, σ^2 is a fraction η of the $\mathrm{RMS}_{\mathrm{signal}}$, that is, $\eta = \sigma^2/\mathrm{RMS}_{\mathrm{signal}}$. Fig. 13 shows strange attractor of the nonlinear pendulum constructed by an ideal time series (free of noise) and a noisy time series with $\eta = 3\%$.

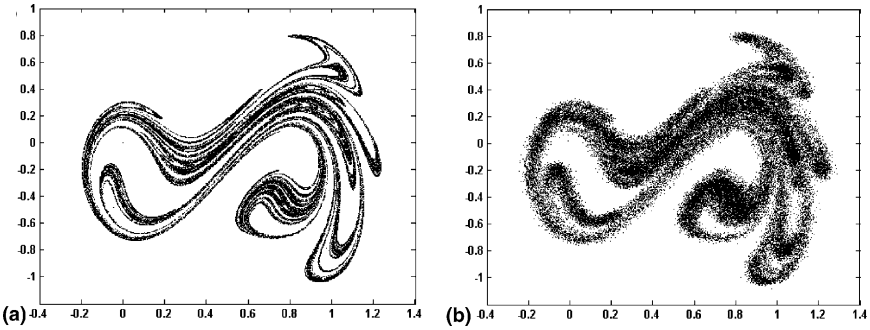

Fig. 13. Strange attractor. (a) Clean. (b) Noise ($\eta = 3\%$).

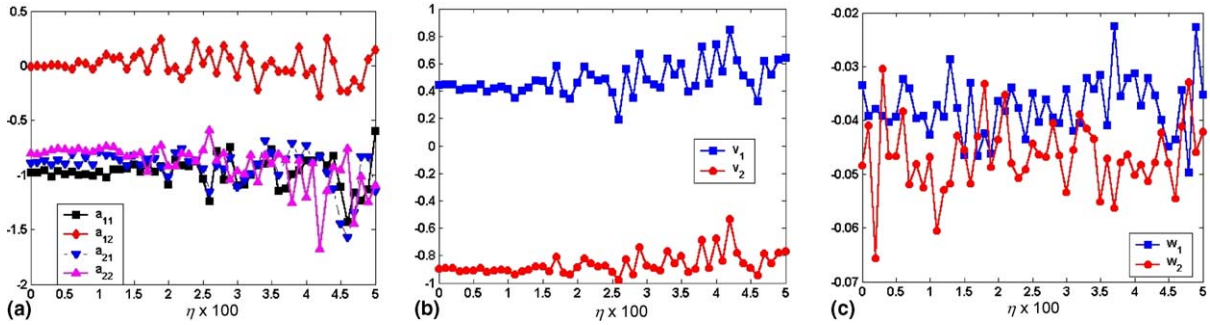

Fig. 14. Influence of noise on control parameters. (a) Jacobian matrix. (b) Maximum contraction vector. (c) Sensitivity vector.

Basically, three different parameters are related to the SCC method: Jacobian matrix, sensitivity vector and maximum contraction direction. Fig. 14 shows these parameters as a function of noise level. Notice that the increase of noise level causes an oscillatory behavior of these parameters. For noise levels with $\eta > 1.5\%$, there is a great level of uncertainties that can cause problems in SCC method efficiency for control purposes. Moreover, it is important to observe the high influence of noise associated with the estimation of the sensitivity vector.

At this point, the sensitivity of the system to perturbations on the control parameter, $\delta p = \Delta l$, is considered. With this aim, two different initial conditions are considered and, for each one, two situations are analyzed: The first considers $\Delta l = 0$ mm, a situation with no control action, while the other assumes $\Delta l = 20$ mm, the maximum value employed for control purposes. These situations simulate variations on the trajectories due to perturbations on the accessible parameter. Fig. 15 shows position evolution and phase space orbit considering two values of control parameter for two different initial conditions, where the actuation starts: $(t, \phi, \dot{\phi}) = (0.82, 1.06, 16.53)$ and $(t, \phi, \dot{\phi}) = (0.41, 4.55, -7.07)$. This analysis shows the period of time necessary for the control parameter affect the system response. Notice that before 20 steps, the effect of control parameter is very small and, after 60 steps, there is a significant divergence between orbits. This behavior allows one to evaluate the optimum number of control stations that manage the compromise between robustness, as diminishing the effects of wrong perturbations, and the ability to stabilize the system, as putting the system on the desired state. This optimum number of control stations is related to the time response of the system.

The forthcoming analysis concerns to the effect of noise on the stabilization of a UPO. The increase of control stations is a useful procedure in order to avoid the effect of noise; however, it is limited by the time response of the system as discussed earlier. In order to study this behavior, an analysis based on a period-3 unstable orbit is carried out.

The increase of the number of control stations causes an increase in the value of control parameter. This behavior is related to the time response of the system. In order to compensate the decrease in the distance between two subsequent control stations, greater values of control parameters are needed. Fig. 16 illustrates this behavior showing control parameters related to the stabilization of the period-3 orbit, for different number of control stations.

Fig. 17 presents a curve of the average of the control perturbation imposed to the system in order to stabilize an unstable orbit as a function of number of control stations, considering different noise levels. Notice that the increase of

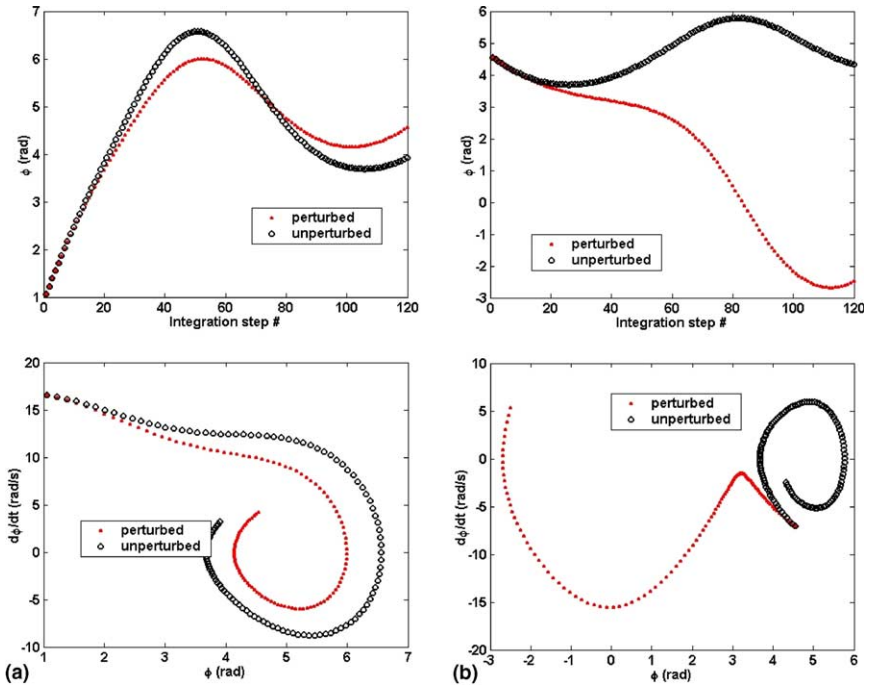

Fig. 15. Sensitivity to control parameter for different initial conditions. (a) $(t, \phi, \dot{\phi}) = (0.82, 1.06, 16.53)$. (b) $(t, \phi, \dot{\phi}) = (0.41, 4.55, -7.07)$.

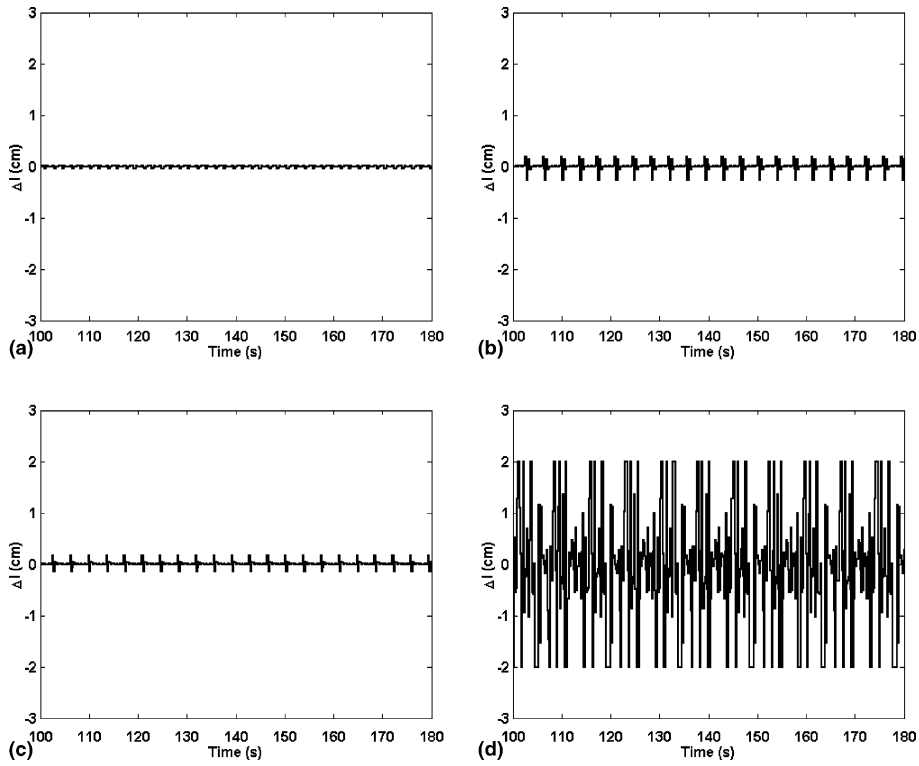

Fig. 16. Control perturbation for different number of control stations. (a) $N = 3$. (b) $N = 4$. (c) $N = 5$. (d) $N = 6$.

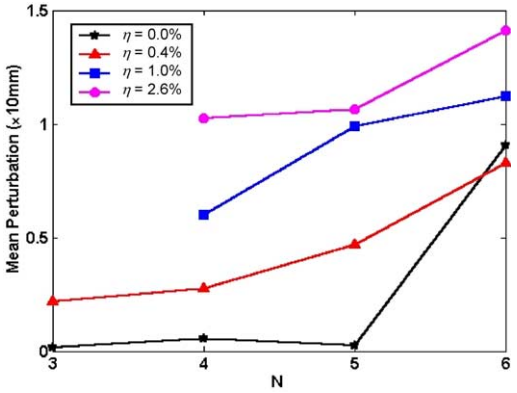

Fig. 17. Average of the control perturbation imposed to the system in order to stabilize an unstable orbit as a function of number of control stations.

the number of control stations tends to cause greater values of control parameters. Moreover, as noise level increases, it is necessary to increase the number of control station in order to control process become effective. Therefore, it is necessary to establish an optimum number of control stations, which is a function of noise and the time response of the system.

At this point, the noise effect on the stabilization of the period-3 orbit is discussed. Different noise levels and number of control stations are considered. Firstly, a noise level $\eta = 0.6\%$ is treated. Fig. 18 presents results related to the stabilization of the desirable orbit showing that, for this noise level, 3 control stations are sufficient to the stabilization. Moreover, it should be pointed out that the same results can be obtained for $N = 4$, 5 and 6.

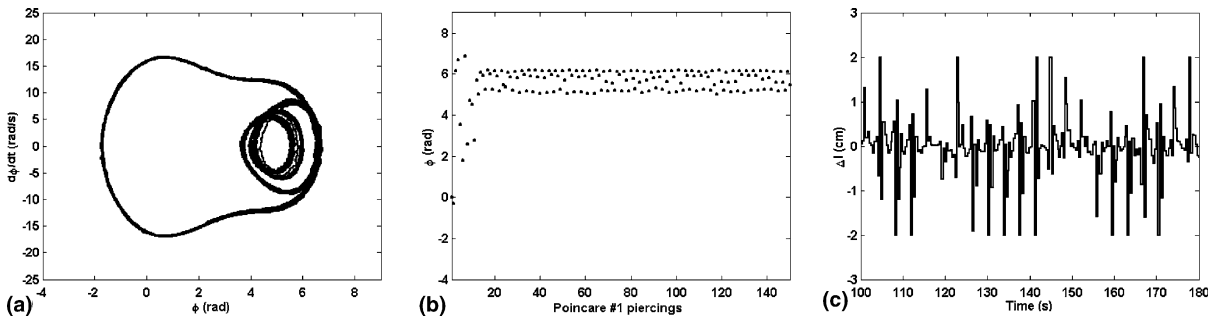

Fig. 18. Stabilization procedure for $\eta = 0.6\%$ with $N = 3$. (a) State space. (b) Position on Poincaré section. (c) Control perturbation.

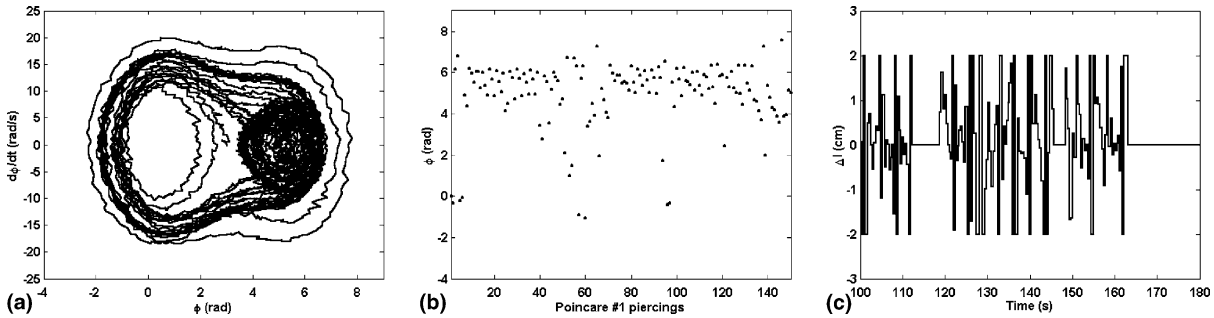

Fig. 19. Stabilization procedure for $\eta = 2.2\%$ with $N = 3$. (a) State space. (b) Position on Poincaré section. (c) Control perturbation.

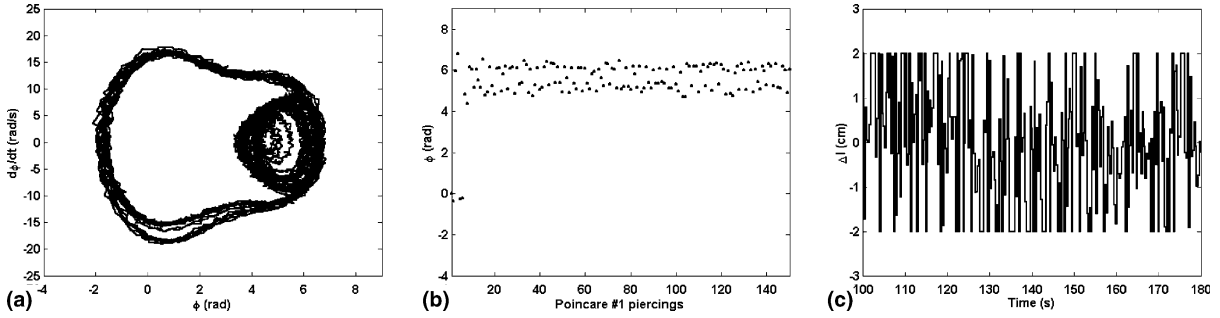

Fig. 20. Stabilization procedure for $\eta = 2.2\%$ with $N = 4$. (a) State space. (b) Position on Poincaré section. (c) Control perturbation.

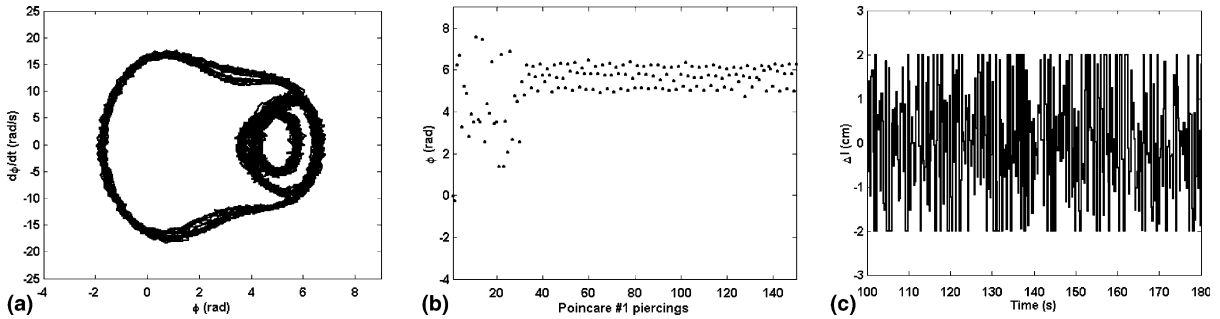

Fig. 21. Stabilization procedure for $\eta = 2.2\%$ with $N = 5$. (a) State space. (b) Position on Poincaré section. (c) Control perturbation.

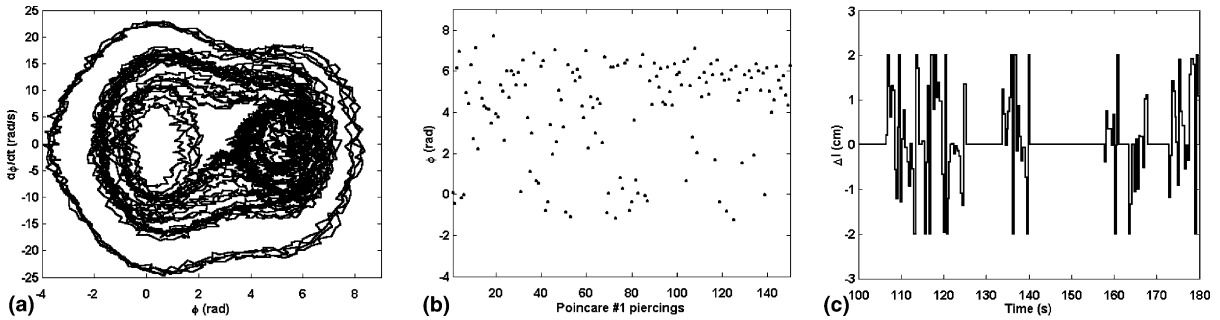

Fig. 22. Stabilization procedure for $\eta = 3.6\%$ with $N = 3$. (a) State space. (b) Position on Poincaré section. (c) Control perturbation.

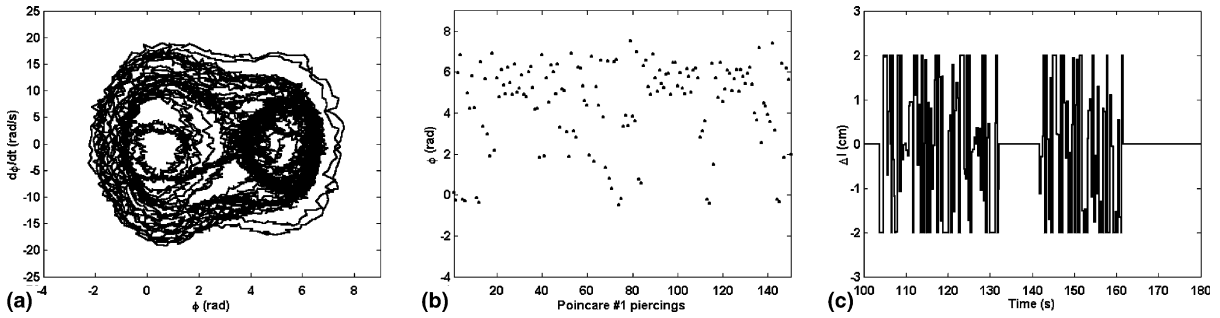

Fig. 23. Stabilization procedure for $\eta = 3.6\%$ with $N = 4$. (a) State space. (b) Position on Poincaré section. (c) Control perturbation.

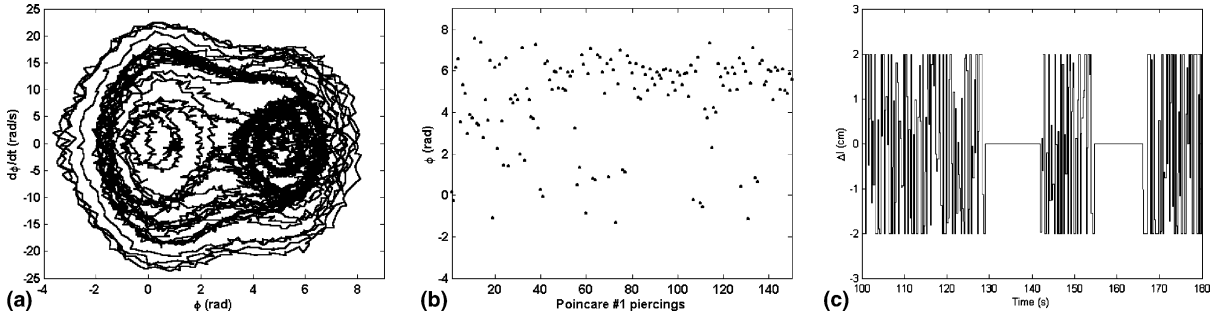

Fig. 24. Stabilization procedure for $\eta = 3.6\%$ with $N = 5$. (a) State space. (b) Position on Poincaré section. (c) Control perturbation.

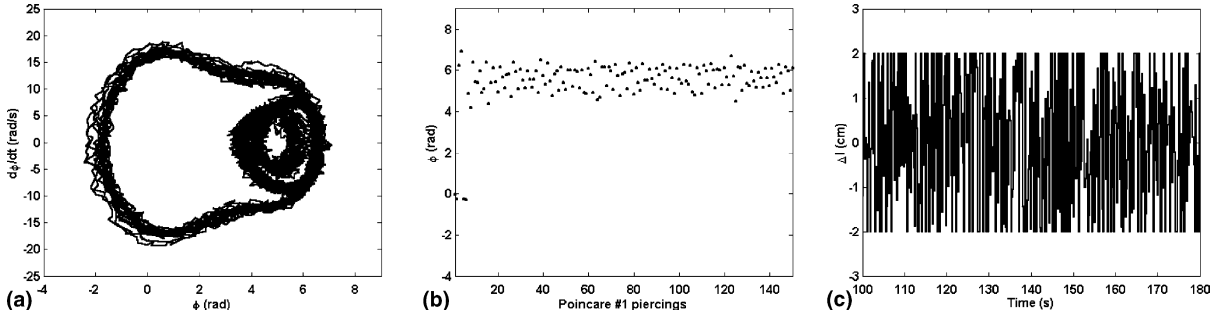

Fig. 25. Stabilization procedure for $\eta = 3.6\%$ with $N = 6$. (a) State space. (b) Position on Poincaré section. (c) Control perturbation.

Now, the noise level is increased for $\eta = 2.2\%$. Under this condition, the increase of the number of control stations becomes important in order to obtain a more effective stabilization of the system, as can be seen in Figs. 19–21.

By increasing even more the noise level for $\eta = 3.6\%$, the influence of the number of control stations is more pronounced. Figs. 22–25 present the process of stabilization for this noisy time series, showing the difficult related to this procedure. It should be pointed out that the stabilization is only effective for $N = 6$. For small number of control stations, the control procedure fails and the system diverges to other orbits.

7. Conclusions

This contribution discusses the control of chaos in a simulated nonlinear pendulum based on an experimental apparatus previously analyzed by Franca and Savi [18] and Pinto and Savi [32]. In the first stage of the control process, the close-return method is employed to identify unstable periodic orbits (UPOs) embedded in the chaotic attractor. After that, the semi-continuous control (SCC) method is considered to stabilize desirable orbits. Least-square fit method is employed to estimate Jacobian matrixes and sensitivity vectors. Moreover, SVD decomposition is employed to estimate directions of unstable and stable manifolds in the vicinity of control points. Signals are generated by the numerical integration of the mathematical model. At first, it is considered that all variables are known. Simulations of control procedure show that SCC method is capable to perform stabilization of the nonlinear pendulum. After that, the analysis is done selecting a single variable as a time series and therefore, it is important to evaluate the effect of delay coordinates method for state space reconstruction. These techniques are employed to stabilize some of the identified UPOs, confirming the possibility of using such approach to control chaotic behavior in mechanical systems using state space reconstruction. Finally, an analysis related to the effect of noise in controlling chaos is of concern. The stabilization of orbits related to noisy time series is more complex and the increase of control stations tends to increase the robustness of the control procedure. Nevertheless, it is important to notice that time response plays an important role in the control procedure, defining the maximum number of control stations.

Acknowledgement

The authors acknowledge the support of the Brazilian Research Council CNPq.

References

[1] Auerbach D, Cvitanovic P, Eckmann J-P, Gunaratne G, Procaccia I. Exploring chaotic motion through periodic orbits. Phys Rev Lett 1987;58(23):2387–9.
[2] Bayly PV, Virgin LN. Practical considerations in the control of chaos. Phys Rev E 1994;50(1):604–7.
[3] Boccaletti S, Grebogi C, Lai Y-C, Mancini H, Maza D. The control of Chaos: Theory and applications. Phys Rep 2000;(329): 103–97.
[4] Bröcker J, Parlitz U, Ogorzalek M. Nonlinear noise reduction. Proc IEEE 2002;90(5):898–918.
[5] Chanfreau P, Lyyjynen H. Viewing the efficiency of chaos control. J Nonlinear Math Phys 1999;6(3):314–31.
[6] Chen G. Introduction to chaos control and anti-control. In: Leung TP, Qin H-S, editors. Advanced Topics in Nonlinear Control Systems. Singapore: World Scientific Pub. Co; 2001. p. 193–245 [Chapter 6].
[7] Christini DJ, Collins JJ, Linsay PS. Experimental control of high-dimensional chaos: The driven double pendulum. Phys Rev E 1996;54(5):4824–7.
[8] Davidchack RL, Lai Y-C. Efficient algorithm for detecting unstable periodic orbits in chaotic systems. Phys Rev E 1999;60(5):6172–5.
[9] Davies M. Noise reduction schemes for chaotic time series. Physica D 1994;79:174–92.
[10] Dhamala M, Lai Y-C, Kostelich EJ. Detecting unstable periodic orbits from transient chaotic time series. Phys Rev E 2000;61(6):6485–9.
[11] Diakonos FK, Schmelcher P, Biham O. Systematic computation of the least unstable periodic orbits in chaotic attractors. Phys Rev Lett 1998;81(20):4349–52.
[12] Ditto WL, Rauseo SN, Spano ML. Experimental control of chaos. Phys Rev Lett 1990;65(26):3211–4.
[13] Ditto WL, Spano ML, Lindner JF. Techniques for the control of chaos. Physica D 1995;86:198–211.
[14] Ditto WL, Showalter K. Introduction: Control and synchronization of chaos. Chaos 1997;7(4):509–11.
[15] Dressler U, Nitsche G. Controlling chaos using time delay coordinates. Phys Rev Lett 1992;68(1):1–4.
[16] Dubé LJ, Després P. The control of dynamical systems—recovering order from chaos. In: Itikawa Y, editor. The Physics of Electronic and Atomic Collisions. AIP Conference Proceedings, 500. 2000. p. 551–70.
[17] Enge N, Buzug Th, Pfister G. Noise reduction on Chaotic attractors. Phys Lett A 1993;175:178–86.
[18] Franca LFP, Savi MA. Distinguishing periodic and chaotic time series obtained from an experimental nonlinear pendulum. Nonlinear Dyn 2001;26:253–71.
[19] Fraser AM, Swinney HL. Independent coordinates for strange attractors from mutual information. Phys Rev A 1986;33:1134–40.
[20] Grebogi C, Lai Y-C. Controlling chaotic dynamical systems. Syst Control Lett 1997;31:307–12.
[21] Gunaratne G, Linsay PS, Vinson MJ. Chaos beyond onset: A comparison of theory and experiment. Phys Rev Lett 1989;63(1): 1–4.
[22] Hübinger B, Doerner R, Martienssen W, Herdering M, Pitka R, Dressler U. Controlling chaos experimentally in systems exhibiting large effective Lyapunov exponents. Phys Rev E 1994;50(2):932–48.
[23] In V, Ditto WL, Spano ML. Adaptative control and tracking of chaos in a magnetoelastic ribbon. Phys Rev E 1995;51(4, part A):R2689–92.
[24] Korte RJ, de Schouten JC, van den Bleek CMV. Experimental control of a chaotic pendulum with unknown dynamics using delay coordinates. Phys Rev E 1995;52(4):3358–65.
[25] Kostelich EJ, Schreiber T. Noise reduction in chaotic time-series data: A survey of common methods. Phys Rev E 1993;48(3):1752–63.
[26] Lefebvre T, Bruyninckx H, De Schutter J. Kalman filters for nonlinear systems: A comparison of performance, Internal Report 01R033, Department of Mechanical Engineering, Katholieke Universiteit Leuven, Belgium, October 2001.
[27] Leung H, Zhu Z, Ding Z. An aperiodic phenomenon of the extended Kalman filter in filtering noisy Chaotic signals. IEEE Trans Signal Process 2000;48(6):1807–10.
[28] Ogorzalek M. Chaos control: How to avoid chaos or take advantage of It. J Franklin Inst 1994;331(6):681–704.
[29] Otani M, Jones AJ. Guiding Chaotic Orbits, 130, Research Report, Imperial College of Science Technology and Medicine, London, 1997.
[30] Ott E, Grebogi C, Yorke JA. Controlling chaos. Phys Rev Lett 1990;64(11):1196–9.
[31] Pawelzik K, Schuster HG. Unstable periodic orbits and prediction. Phys Rev A 1991;43(4):1808–12.
[32] Pinto EGF, Savi MA. Nonlinear prediction of time series obtained from an experimental pendulum. Current Top Acoust Res—Res Trends, in press.
[33] Pierson D, Moss F. Detecting periodic unstable points in noisy chaotic and limit cycle attractor with application to biology. Phys Rev Lett 1995;75(11):2124–7.
[34] Pingel D, Schmelcher P, Diakonos FK, Biham O. Theory and applications of the systematic detection of unstable periodic orbits in dynamical systems. Phys Rev E 2000;62(2):2119–34.

[35] Pyragas K. Continuous control of chaos by self-controlling feedback. Phys Lett A 1992;170:421–8.
[36] Ritz T, Schweinsberg ASZ, Dressler U, Doerner R, Hübinger B, Martienssen W. Chaos control with adjustable control times. Chaos Solitons & Fractals 1997;8(9):1559–76.
[37] Rhodes C, Morari M. False-nearest-neighbors algorithm and noise-corrupted time series. Phys Rev E 1997;55(5):6162–70.
[38] Sauer T. A noise reduction method for signals from nonlinear systems. Physica D 1992;58:193–201.
[39] Schmelcher P, Diakonos FK. Detecting unstable periodic orbits of chaotic dynamical systems. Phys Rev Lett 1997;78(25):4733–6.
[40] Schmelcher P, Diakonos FK. General approach to the localization of unstable periodic orbits in Chaotic dynamical systems. Phys Rev E 1998;57(3):2739–46.
[41] Shin K, Hammond JK, White PR. Iterative SVD method for noise reduction of low-dimensional chaotic time-series. Mech Syst Signal Process 1999;13(1):115–24.
[42] Shinbrot T, Grebogi C, Ott E, Yorke JA. Using small perturbations to control chaos. Nature 1993;363:411–7.
[43] Schreiber T, Grassberger P. A simple noise-reduction method for real data. Phys Lett A 1991;160:411–8.
[44] Schreiber T, Richter M. Fast nonlinear projective filtering in a data stream. Int J Bifurcat Chaos 1999;9(10):2039–45.
[45] So P, Ott E. Controlling chaos using time delay coordinates via stabilization of periodic orbits. Phys Rev E 1995;51(4):2955–62.
[46] So P, Ott E, Schiff S, Kaplan DT, Sauer T, Grebogi C. Detecting unstable periodic orbits in chaotic experimental data. Phys Rev Lett 1996;76(25):4705–8.
[47] Starret J, Tagg R. Control of a Chaotic parametrically driven pendulum. Phys Rev Lett 1995;74(11):1974–7.
[48] Takens F. Detecting strange attractors in turbulence. In: Rand DA, Young LS, editors, Proceedings of the Symposium on Dynamical Systems and Turbulence, University of Warwick, 1979–1980, Berlin: Springer; 1981.
[49] Yagasaki K, Uozumi T. Controlling chaos in a pendulum subjected to feedforward and feedback control. Int J Bifurcat Chaos 1997;7(12):2827–35.
[50] Wan EA, van der Merwe R. The unscented Kalman filter. In: Haykin S, editor. Kalman Filtering and Neural Networks. Wiley Publ; 2001.
[51] Wang R, Jing Z. Chaos control of chaotic pendulum system. Chaos, Solitons & Fractals 2004;21:201–7.
[52] Wolf A, Swift JB, Swinney HL, Vastano JA. Determining Lyapunov exponents from a time series. Physica D 1985;16:285–317.
[53] Spano ML, Ditto WL, Rauseo SN. Exploitation of chaos for active control: An experiment. Journal of Intelligent Materials Systems and Structures 1991;2:482–93.
[54] Pei X, Dolan K, Moss F, Lai YC. Counting unstable periodic orbits in noisy chaotic systems: A scaling relation connecting experiment with theory. Chaos 1998;8(4):853–60.
[55] Dolan K, Witt A, Spano ML, Neiman A, Moss F. Surrogates for finding unstable periodic orbits in noisy data sets. Physical Review E 1999;59(5):5235–41.
[56] Dolan K. Extracting dynamical structure from unstable periodic orbits. Physical Review E 2001;64(2), Art No. 026213.